Examining the interdependence and cooperation of the terms in the distinct inverse scattering subseries for free-surface multiple and internal multiple removal

Chao Ma and Arthur B. Weglein, M-OSRP/Physics Dept./University of Houston*

SUMMARY

The Inverse Scattering Series (ISS) contains task specific subseries that achieve objectives associated with inversion. In this paper, we examine the subseries for free-surface multiple and internal multiple removal. We define the purpose of the individual terms in these subseries and show that what might appear to be a local weakness or deficit when examining that term in isolation, is, in fact, a purposeful activity within the overall objective of the subseries. This property of purposeful perturbation is a consequence of the fact that the inverse scattering series is a direct inversion method. Every term in a task specific subseries has a well-defined purpose and is always positive and helpful when considering the overall purpose and objective of the task specific subseries. We explain and illustrate how that property has important conceptual and practical consequences.

INTRODUCTION

Scattering theory is a form of perturbation analysis; it describes how a perturbation in the properties of a medium relates a perturbation to a wavefield that experiences that perturbed medium (Weglein et al., 2003). It is customary to consider the original unperturbed medium as the reference medium. The difference between the actual and reference media is characterized by the perturbation operator. The corresponding difference between the actual and reference wavefields is called the scattered wavefield. Forward scattering takes as input the reference medium, the reference wavefield and the perturbation operator and outputs the actual wavefield. Inverse scattering takes as input the reference medium, the reference wavefield and values of the actual field on the measurement surface and outputs the difference between actual and reference medium properties through the perturbation operator.

Inverse Scattering Series methods were first developed by Moses (1956), Prosser (1969) and Razavy (1975) and were transformed for application to a multi-dimensional earth and exploration seismic reflection data by Weglein et al. (1981) and Stolt and Jacobs (1980). The important pioneering work on convergence criteria for the inverse scattering series (Prosser, 1969) provides a condition which is difficult to translate into a statement on the size and duration of the contrast between actual and reference media. Carvalho (1992) performed empirical tests for a 1D acoustic medium without any subsurface information. The result indicated the full series only convergences when the difference between the actual earth's acoustic velocity and reference velocity (water velocity) is less than 11%.

An apparent lack of robust convergence* of the overall series suggested by numerical tests motivates the concept that inversion can be viewed as a set of steps where each step is achieved by different, task-specific subseries corresponding to that specific task (Weglein et al., 2003). For example, each step in inversion can be defined as achieving a task or objective: (1) removing free-surface multiples (2) removing internal multiples; (3) locating and imaging reflectors in space; and (4) determining the changes in earth material properties across those reflectors. The idea was to identify, within the overall series, specific distinct subseries that performed these focused tasks and to evaluate these subseries for convergence, requirements for a priori information, rate of convergence, data requirements and theoretical and practical prerequisites. It was imagined (and hoped) that perhaps a subseries for one specific task would have a more favorable attitude towards, e.g., convergence in comparison to the entire series.

Within each subseries, every term plays specific roles and different terms within the same subseries work in a cooperative way towards achieving the task associated with that subseries. The property of each term playing specific tasks and different terms working collectively are referred to as purposeful perturbation (Weglein et al., 2003). The concept of purposeful perturbation not only has significant practical applications (e.g., in the ISS free-surface multiple elimination algorithm, it determines how many terms are required based on how many orders of free-surface multiples are significant and need to be removed) but also has tremendous implications on how ISS works toward achieving seismic processing goals. Hence, a thorough understanding of what task can be achieved by each term in a specific subseries provides guidance for its practical use. In addition, a knowledge of the role that each term plays in a specific subseries allows us to better understand the series and further identify/isolate more terms from the series to provide more capabilities.

Based on previous works of Araujo et al. (1994), Weglein et al. (1997, 2003) and Zhang and Shaw (2010), we extend our understanding of purposeful perturbation in the the ISS internal multiple attenuation algorithm in this paper. We will first review an example of purposeful perturbation in the ISS free-surface multiple elimination algorithm from Weglein et al. (2003), and compare the similarities and differences between these two cases.

EXAMPLE OF PURPOSE PERTURBATION IN THE ISS FREE-SURFACE MULTIPLE REMOVAL CASE

Following Weglein et al. (2003), we illustrate the purposeful perturbation in ISS free-surface removal case using a 1D nor-

*There are other factors that motivate the idea of developing distinct and task-specific subseries. See Weglein et al. (2003) for more details.

mal incident example. In a 1D earth with a normal incident plane wave and a source wavelet with a unit amplitude, the ISS free-surface multiple removal algorithm can be written as:

$$\begin{aligned} R =& \frac{R_{FS}}{1-R_{FS}} \\ =& R_{FS} + R_{FS}^2 + R_{FS}^3 + \cdots, \end{aligned} \tag{1}$$

where R_{FS} and R are data with and without free-surface multiples, respectively. Notice that the free-surface is characterized by a reflection coefficient of -1 for a pressure wavefield. Subsequent terms on the right hand side of equation 1 (e.g., R_{FS}^2 and R_{FS}^3) are free-surface multiple predictions from the ISS. Adding the predictions to the data provides the data without free-surface multiples (i.e., R).

We use a 1D analytic example to illustrate the prediction of the free-surface multiples. The model (Figure 1) has two reflectors, and the input data with two primaries, three first-order (blue terms) and four second-order (red terms) free-surface multiples, can be written as:

$$\begin{aligned} R_{FS}(t) =& R_1\delta(t-t_1) + R_2'\delta(t-t_2) - R_1^2\delta(t-2t_2) - R_2'^2\delta(t-2t_2) \\ & -2R_1R_2'\delta(t-t_1-t_2) + R_1^3\delta(t-3t_1) + R_2'^3\delta(t-3t_2) \\ & +3R_1R_2'^2\delta(t-t_1-2t_2) + 3R_1^2R_2'\delta(t-2t_1-t_2) + \cdots, \end{aligned} \tag{2}$$

where R_1 and $R_2'(=T_{01}R_2T_{10})$ are amplitudes of the first and second primaries, respectively. R_1 and R_2 are reflection coefficients corresponding to the first and second reflector, T_{01} and T_{10} are transmission coefficients across the first reflector. We have assumed the downward reflection coefficient at the free-surface to be -1.

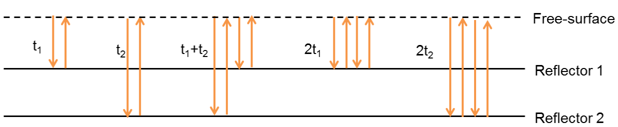

Figure 1: A one dimensional model with two reflectors. There are two primaries and three first-order free-surface multiples shown in the figure.

In the temporal frequency domain, the data are

$$\begin{aligned} R_{FS}(\omega) =& R_1e^{i\omega t_1} + R_2'e^{i\omega t_2} - R_1^2e^{i\omega 2t_1} - R_2'^2e^{i\omega 2t_2} \\ & -2R_1R_2'e^{i\omega(t_1+t_2)} + R_1^3e^{i\omega 3t_1} + R_2'^3e^{i\omega 3t_2} + 3R_1^2R_2'e^{i\omega(2t_1+t_2)} \\ & +3R_1R_2'^2e^{i\omega(t_1+2t_2)} + \cdots. \end{aligned} \tag{3}$$

With equation 3, the second and third terms in equation 1 are

$$\begin{aligned} R_{FS}^2(\omega) =& R_1^2e^{i\omega 2t_1} + R_2'^2e^{i\omega 2t_2} + 2R_1R_2'e^{i\omega(t_1+t_2)} \\ & -6R_1R_2'^2e^{i\omega(t_1+2t_2)} - 6R_1^2R_2'e^{i\omega(2t_1+t_2)} \\ & -2R_1^3e^{i\omega 3t_1} - 2R_2'^3e^{i\omega 3t_2} + \cdots, \end{aligned} \tag{4}$$

and

$$\begin{aligned} R_{FS}^3(\omega) =& R_1^3e^{i\omega 3t_1} + R_2'^3e^{i\omega 3t_2} + 3R_1R_2'^2e^{i\omega(t_1+2t_2)} \\ & +3R_1^2R_2'e^{i\omega(2t_1+t_2)} + \cdots, \end{aligned} \tag{5}$$

respectively.

From equation 4, we can conclude that (Weglein et al., 2003) when $R_{FS}^2(\omega)$ is added to $R_{FS}(\omega)$, two things happen: (1) the first-order free-surface multiples are eliminated (blue terms in equations 3 and 4 cancel each other) and (2) higher-order free-surface multiples are altered. Together with $R_{FS}^3(\omega)$, second-order free-surface multiples are eliminated (red terms in equations 3, 4 and 5 cancel each other) as shown in equation 6.

$$\begin{aligned} R_{FS}(\omega): &\quad 1\times[R_1^3e^{i\omega 3t_1} + R_2'^3e^{i\omega 3t_2} + 3R_1^2R_2'e^{i\omega(2t_1+t_2)} + 3R_1R_2'^2e^{i\omega(t_1+2t_2)}] \\ R_{FS}^2(\omega): &\quad -2\times[R_1^3e^{i\omega 3t_1} + R_2'^3e^{i\omega 3t_2} + 3R_1^2R_2'e^{i\omega(2t_1+t_2)} + 3R_1R_2'^2e^{i\omega(t_1+2t_2)}] \\ R_{FS}^3(\omega): &\quad 1\times[R_1^3e^{i\omega 3t_1} + R_2'^3e^{i\omega 3t_2} + 3R_1R_2'^2e^{i\omega(t_1+2t_2)} + 3R_1^2R_2'e^{i\omega(2t_1+t_2)}] \end{aligned} \tag{6}$$

The alteration in $R_{FS}^2(\omega)$ **prepares** for the elimination of second-order free-surface multiples using $R_{FS}^3(\omega)$.

Next, we further categorize the results as follows. Consider the input data containing primary and free-surface multiples, i.e.,

$$R_{FS}(\omega) = P + F,$$

where P and F stand for primaries and free-surface multiples, respectively.

Therefore, $R_{FS}^2(\omega)$ can be expressed as

$$R_{FS}^2(\omega) = (P+F)^2 = PP + PF + FP + FF.$$

Under this categorization, the blue and red terms in equation 4 come from combinations of PP and PF (or FP) terms, respectively. Together with the 1D analytic example, we conclude that the PP combination in $R_{FS}^2(\omega)$ is used to eliminate the first-order free-surface multiples, whereas the PF (or FP) combination in $R_{FS}^2(\omega)$ is used to alter and benefit the elimination of the second-order free-surface multiples.

In this section, with the 1D analytic example, the ISS free-surface elimination algorithm demonstrates the collaborative nature among the different terms to **collectively fulfill** the task. The ISS free-surface-multiple elimination algorithm anticipates that there are both primaries and free-surface multiples as input and uses both of them to achieve that task. In the next section, we will use a two-reflector example to discuss an analogous feature in the ISS internal-multiple-attenuation case, and we will analyze the difference between these two cases.

EXAMPLE OF PURPOSEFUL PURTURBATION IN THE ISS INTERNAL MULTIPLE ATTENUATION CASE

In this section, we will use a normal incident example in a 1D earth to illustrate the cooperative nature between different terms in ISS internal multiple attenuation algorithm.

A 1D version of the ISS internal-multiple-attenuation algorithm is shown in equation 7

$$D'(t) = D(t) + D_3(t) + D_5(t) + \cdots, \tag{7}$$

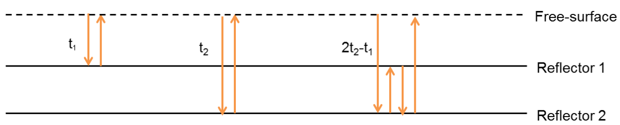

Figure 2: A one dimensional model with two reflectors. There are two primaries and one first-order internal multiple shown in the figure.

$D(t)$ on the right hand side of equation 7 is the input data set which consists of primaries and internal multiples, $D_3(t)$, $D_5(t)$ and subsequent terms (represented by "$\cdots$" in equation 7) are terms identified and isolated from inverse scattering series with each term having specific roles in attenuating internal multiples in the data. For example, $D_3(t)$ has the role of (1) predicting all the first-order internal multiples (used to attenuate the first-order internal multiples in the data) and (2) predicting all higher-order internal multiples (used to benefit attenuating higher-order internal multiples in the data, as this paper will show in the following). $D'(t)$ on the left hand side is the data after internal multiple attenuation.

The reflection data due to an impulsive incident wave for a two reflector model (see Figure 2) are

$$D(t) = R_1\delta(t-t_1) + R_2'\delta(t-t_2) + R_4'\delta(t-(2t_2-t_1)) + \cdots, \tag{8}$$

where $R_2' = T_{01}R_2T_{10}$, and $R_4' = T_{01}R_2(-R_1)R_2T_{10}$ (R_1, R_2, T_{01} and T_{10} have the same meaning as in equation 2). Note that we include internal-multiples in the data.

To obtain $D_3(t)$ in equation 7, we first apply a temporal Fourier transform on $D(t)$,

$$D(\omega) = R_1e^{i\omega t_1} + R_2'e^{i\omega t_2} + R_4'e^{i\omega(2t_2-t_1)} + \cdots. \tag{9}$$

For a 1D medium and a normal incident plane wave, $D(\omega) = b_1(k)$ and the vertical wave number is $k = \frac{2\omega}{c_0}$. Then, the reflection data can be expressed in terms of k,

$$b_1(k) = R_1e^{i(\frac{2\omega}{c_0})(\frac{c_0t_1}{2})} + R_2'e^{i(\frac{2\omega}{c_0})(\frac{c_0t_2}{2})} + R_4'e^{i(\frac{2\omega}{c_0})(\frac{c_0(2t_2-t_1)}{2})} + \cdots. \tag{10}$$

Define the pseudo-depths z_1 and z_2 in the reference medium as $z_1 \equiv \frac{c_0t_1}{2}$ and $z_2 \equiv \frac{c_0t_2}{2}$, respectively. Rewrite the data as,

$$b_1(k) = R_1e^{ikz_1} + R_2'e^{ikz_2} + R_4'e^{ik(2z_2-z_1)} + \cdots. \tag{11}$$

After performing the Inverse Fourier transform from k to z, $b_1(z) = \int_{-\infty}^{\infty} e^{-ikz}b_1(k)dz$, substituting the data into the algorithm $b_3(k) = \int_{-\infty}^{\infty} dz_1e^{ikz_1}b_1(z_1)\int_{-\infty}^{z_1-\varepsilon} dz_2e^{-ikz_2}b_1(z_2)\int_{z_2+\varepsilon}^{\infty} dz_3e^{ikz_3}b_1(z_3)$, where ε is a small positive number, and Fourier transforming back to the time domain (in this case, $b_3(k) = D_3(\omega)$), we have

$$D_3(t) = R_1R_2'^2\delta(t-(2t_2-t_1)) + 2R_1R_2'R_4'\delta(t-(3t_2-2t_1)) + R_2'R_4'^2\delta(t-(3t_2-2t_1)) + R_1R_4'^2\delta(t-(4t_2-3t_1)). \tag{12}$$

Equation 12 shows that the prediction includes (1) the first-order internal multiples (the blue term) and (2) higher-order internal multiples (the red terms).

Also, to categorize the result, consider the input data containing primary and internal multiples, i.e.,

$$b_1 = P + I,$$

where P and I stand for primaries and internal multiples, respectively. The prediction result of the attenuator of the first-order internal multiples is

$$\begin{aligned} b_3 &= b_1 * b_1 * b_1 \\ &= (P+I)(P+I)(P+I) \\ &= PPP + PPI + PIP + IPP + PII + IPI + IIP + III. \end{aligned} \tag{13}$$

Further analysis shows that the prediction of the first-order internal multiples (the blue term in equation 12) results from *PPP* combinations and prediction of all other higher-order internal multiples (red terms in equation 12) results from *PPI* (or *IPP* or *IPI*) combinations.

To summarize analogous points in the free-surface multiple and internal multiple cases: (1) both first-order and higher-order multiples are predicted in $R_{FS}^2(\omega)$ and b_3; and (2) higher-order multiples are predicted because of the lower-order multiples in the input data entering as subevents.

HIGHER-ORDER INTERNAL MULTIPLES PREDICTED IN B_3

In section 2, it was shown that the second-order free-surface multiples predicted by $R_{FS}^2(\omega)$ are used to eliminate the second-order free-surface multiple (see equation 6). Next, we will show the second-order internal multiples predicted by D_3 (the first two red terms in 12) will assist and benefit the attenuating of second-order internal multiples in the seismic data.

We first examine the prediction of ISS attenuator of the second-order internal multiples (Araujo et al., 1994), i.e.,

$$b_5(k) = \int_{-\infty}^{\infty} dz_1e^{ikz_1}b_1(z_1)\int_{-\infty}^{z_1-\varepsilon} dz_2e^{-ikz_2}b_1(z_2)\int_{z_2+\varepsilon}^{\infty} dz_3e^{ikz_3}b_1(z_3) \times \int_{-\infty}^{z_3-\varepsilon} dz_4e^{ikz_4}b_1(z_4)\int_{z_4+\varepsilon}^{\infty} dz_5e^{-ikz_5}b_1(z_5). \tag{14}$$

Given equation 14, the prediction result using the same input data (equation 8) is

$$D_5(t) = R_2'^3R_1^2\delta(t-(3t_2-t_1)) + \cdots = T_{01}^3T_{10}^3R_2^3R_1^1\delta(t-(3t_2-2t_1)) + \cdots. \tag{15}$$

This is the prediction of the second-order internal-multiple from the attenuator of the second-order internal multiples.

To summarize, the actual second-order internal multiple in the data $D(t)$, the second-order internal-multiple prediction in $D_3(t)$, and $D_5(t)$ are

$$\begin{aligned} D(t):&\quad 1\times[T_{01}T_{10}R_2^3R_1^2\delta(t-(3t_2-2t_1))] \\ D_3(t):&\quad (-2T_{01}T_{10}+(T_{01}T_{10}R_1)^2)\times[T_{01}T_{10}R_2^3R_1^2\delta(t-(3t_2-2t_1))] \\ D_5(t):&\quad (T_{01}T_{10})^2\times[T_{01}T_{10}R_2^3R_1^2\delta(t-(3t_2-2t_1))], \end{aligned} \tag{16}$$

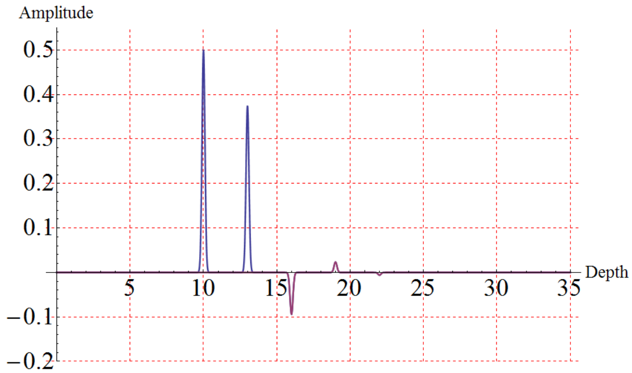

Figure 3: Input data in pseudo-depth domain. **Blue** and **purple** lines represent primaries and internal multiples, respectively. There are two primaries at depths 10 and 13 and three internal multiples at pseudo-depths 16 (first-order), 19 (second-order), and 22 (third-order).

respectively. Comparing equations 6 and 16, we find analogous roles of the higher-order internal-multiple prediction in $D_3(t)$, i.e., the prediction of the second-order internal multiples by $D_3(t)$ **assists and benefits** the attenuating of higher internal multiples in the data. Similar to the ISS free-surface multiple removal case, the ISS internal multiple attenuation algorithm anticipates that both primaries and internal multiples will be the input, and uses both types of events to attenuate internal multiples in the data.

Next, we show a numerical example in 1D case to demonstrate the purposeful perturbation between different terms in the ISS internal multiple attenuation algorithm to collectively achieve the attenuation of internal multiples. Figure 3 shows the test data we use (shown in the pseudo-depth domain). Figure 4, 5 and 6 shows the comparison between the input data (before attenuating internal multiples) and the output data (after attenuating internal multiples) when adding different prediction terms in equation 7.

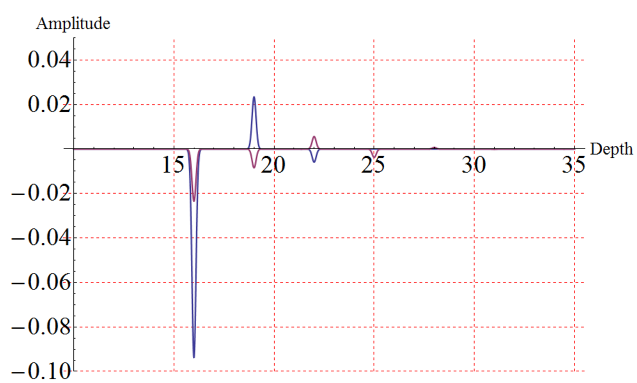

Figure 4: Comparison between D (**blue**) and $D+D_3$ (**purple**). The comparison shows the contributions of D_3 are (1) reducing the first-order internal multiples and (2) altering the amplitude of the higher-order internal multiples. Notice that, only internal multiples are plotted in D.

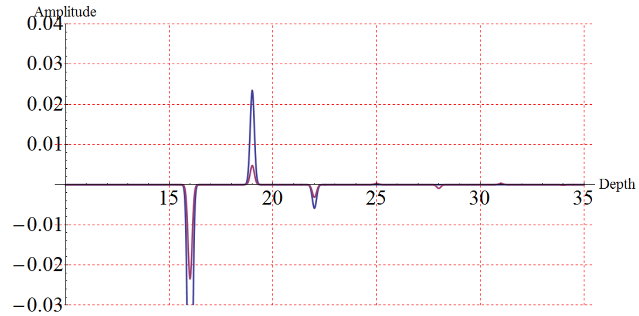

Figure 5: Comparison between D (blue) and $D+D_3+D_5$ (purple). Comparing Figure 4 and 5, it is concluded that adding D_5 to $D+D_3$ will further reduces second-order internal multiple.

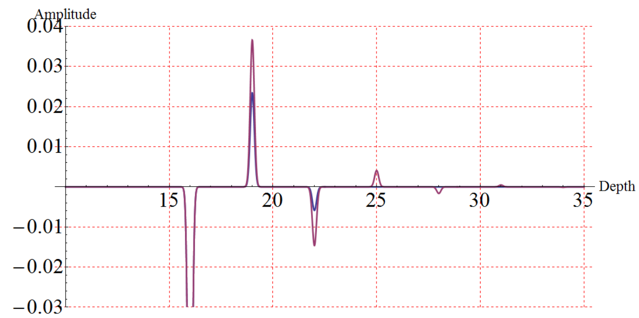

Figure 6: Comparison between D (blue) and $D+D_5$ (purple). Without the contribution from D_3, $D+D_5$ will **increase** the amplitude of the second-order internal multiple. In other words, alteration of higher-order internal multiples by D_3 is necessary for their attenuation.

CONCLUSIONS

In this paper, we use 1D examples to examine the property of purposeful perturbation in the distinct ISS free-surface multiple and internal multiple removal algorithms. The examples shown in this paper demonstrate that terms in the ISS task specific subseries have well-defined purposes and show how different terms work collectively towards achieving seismic processing objective associated with that specific subseries. The study extends our understanding of the series and provide a guide for selecting additional terms for more ambitious inversion objectives and capability.

ACKNOWLEDGMENTS

We are grateful to all M-OSRP sponsors for their encouragement and support of this research.

REFERENCES

Araujo, F. V., A. B. Weglein, P. M. Carvalho, and R. H. Stolt, 1994, Inverse scattering series for multiple attenuation: An example with surface and internal multiples: SEG Technical Program Expanded Abstracts, 1039–1041.

Carvalho, P. M., 1992, Free-surface multiple reflection elimination method based on nonlinear inversion of seismic data: PhD thesis, Universidade Federal da Bahia.

Moses, H., 1956, Calculation of scattering potential from reflection coefficients: Phys. Rev., 559–567.

Prosser, R. T., 1969, Formal solutions of inverse scattering problems: Journal of Mathematical Physics, **10**, 1819–1822.

Razavy, M., 1975, Determination of the wave velocity in an inhomogeneous medium from reflection data: J. Acoust. Soc. Am., **58**, 956–963.

Stolt, R. H., and B. Jacobs, 1980, Inversion of seismic data in a laterally heterogeneous medium: Stanford Exploration Project, **24**.

Weglein, A. B., F. V. Araújo, P. M. Carvalho, R. H. Stolt, K. H. Matson, R. T. Coates, D. Corrigan, D. J. Foster, S. A. Shaw, and H. Zhang, 2003, Inverse scattering series and seismic exploration: Inverse Problems, R27–R83.

Weglein, A. B., W. E. Boyce, and J. E. Anderson, 1981, Obtaining three-dimensional velocity information directly from reflection seismic data: An inverse scattering formalism: Geophysics, **46**, 1116–1120.

Weglein, A. B., F. A. Gasparotto, P. M. Carvalho, and R. H. Stolt, 1997, An inverse-scattering series method for attenuating multiples in seismic reflection data: Geophysics, **62**, 1975–1989.

Zhang, H., and S. Shaw, 2010, 1-d analytical analysis of higher order internal multiples predicted via the inverse scattering series based algorithm: SEG Expanded Abstracts, **29**, 3493–3498.